SURFACE ELECTRONIC STATESTHE CO-NDO METHOD IN REGULAR CHEMISORPTION STUDIES. APPLICATION TO ATOMIC HYDROGEN ON GRAPHITE

F. Ricca

THE CO-NDO METHOD IN REGULAR CHEMISORPTION STUDIES. APPLICATION TO ATOMIC HYDROGEN ON GRAPHITE (*)

F. RICCA

Institute of Theoretical Chemistry, University of Turin, Turin, Italy

Résumé. — On expose la méthode de l'orbitale cristalline dans l'approximation CNDO/2 et on discute le problème de la convergence des sommes sur les mailles du réseau. On donne aussi les expressions pour le calcul de la densité électronique et des densités d'états projetées.

Comme exemple de l'applicabilité de la méthode aux problèmes de la chimisorption régulière, on étudie les différentes phases cristallines qui pourraient se former par chimisorption d'hydrogène atomique sur une mono-couche de graphite. Pour chacune de ces phases, on donne la structure de bandes et les spectres de la densité d'états. Pour la phase la plus stable, qui correspond à une concentration atomique 1/1 de l'hydrogène par rapport au carbone, on donne aussi une description graphique de la distribution de la densité électronique.

Abstract. — The crystalline orbital method in the approximate version of CNDO/2 is illustrated and the problem of truncation in the sums over direct lattice is discussed. Expressions for population analysis and projected densities of states are given.

As an example of the applicability of the method to regular chemisorption problems, different crystal phases that could be formed by chemisorption of atomic hydrogen on a graphite monolayer are examined, by taking into account the substrate relaxation. Band structures and density of states spectra are furnished for all of them and an electron density map is given for the most favoured, which corresponds to a hydrogen/carbon atomic ratio 1/1.

1. **Introduction.** — Adsorption studies may be gathered in two groups depending on the fact that they consider the solid surface as the unique macroscopic defect in the adsorbent, or they pay attention to a number of different microscopic defects in the surface itself. The first approach, recognizing a perfect two-dimensional periodicity to the surface (without edges, vertices, steps, kinks, holes, etc. and without chemical impurities) is better related to experimental structuristic studies as well as to theoretical quantum treatments, while the second one furnishes kinetic and catalytic works with more realistic and more flexible models.

Looking at the substrate as an infinite perfect crystal face, the further liberty remains of considering adsorption as a single event involving just an isolated gaseous particle, or else as a massive process, well based on thermodynamical grounds and generating well defined adsorbed phases with specific stoichiometric and stereochemical features. Here again two different targets are aimed at, the first being principally to characterize the adsorbent, its surface, its possible role in transient phenomena like catalysis and surface reactions, while the second is to characterize the two-dimensional adsorbed phase. The first problem has some analogies with that of point defects in solids, while the second one is more similar to the problem of studying surface electron states, surface reconstruction, epitaxial growth and so on. Both of them can be attacked by the tools of quantum-mechanics. In the case of chemisorption, where electrons are shared between the adsorbent and the adsorbate, these two problems can be treated through the two different approaches of the *surface molecule* variously embedded in the adsorbent matrix, and of the *regular phase* variously structured over the crystal lattice of the adsorbent.

Chemisorption studies of this second kind, which are the object of the present work, have much in common with usual studies on solid state and present the same intrinsic difficulties. However, two particular features have to be considered which, though arising from a complication of this problem, yet seem to legitimate simpler solutions. First, the special interest in characterizing the new chemical bonds formed with different chemical species at the surface of the solid allows some reasonable restrictions to be introduced when considering the adsorbent-adsorbate system. Treating this system as a two-dimensional phase by taking into account a layer only a few atoms thick certainly produces a poor picture of its electron properties, but probably suffices for giving a good picture of essential

(*) This work has been partially financed by the Italian Council of Research.

changes occurring in such properties with chemisorption.

Second, theoretical approaches like the tight-binding method, which proved unable to give a fully satisfactory description of the electron properties of solids, are probably good enough for characterizing the new chemical bonds formed at the surface with an approximation which is comparable to that usually accepted when studying large molecules by the standard methods of quantum chemistry. Furthermore, this approach can produce the important result of maintaining some useful concepts of ordinary chemistry and allowing the different languages of quantum chemistry and solid state physics to be easily translated into each other.

According to this view, it is of importance to maintain the Hartree-Fock scheme generally applied in quantum chemistry, using a typical SCF procedure, without further approximations in evaluating the exchange terms. *Ab initio* HF-SCF calculations of regular chemisorbed phases appear to be feasible in principle, but the computational effort is probably too large in most cases. Restricting to minimal basis sets or to valence electron sets is almost compulsory and employing semi-empirical methods within the HF-SCF scheme may be of assistance. Among such approximate methods, CNDO/2 seems to deserve a special interest because of its good performances in determining geometries, as no direct experimental data for surface conformations are generally available. Caution is needed, of course, about quantitative results obtained with such approximation, but it proves useful for testing hypotheses and models, as well as for setting up computational techniques. In fact CNDO energies, though unrealistic in many cases, can be used properly for comparison purposes.

The simplest conceivable realistic example of regular chemisorption which can be studied in this way is perhaps the adsorption of atomic hydrogen on a graphite monolayer, as the adsorbed species may be characterized by a single 1 s AO, while the adsorbent is strictly two-dimensional and composed of a single kind of atoms. Taking advantage of the experience acquired with this simple case, further steps can be envisaged both towards more complex adsorbates and towards thicker adsorbing layers.

2 **The CO-NDO method.** — A crystalline orbital for an infinite lattice [1-3] is approximated by a linear combination ψ of tight-binding Bloch functions φ, each corresponding to an atomic orbital χ:

$$\psi_j^{\mathbf{k}}(\mathbf{x}) = \sum_R \sum_\rho a_{\rho j}^{\mathbf{k}} \varphi_\rho^{\mathbf{k}}(\mathbf{x}) \tag{1}$$

$$\varphi_\rho^{\mathbf{k}}(\mathbf{x}) = N^{-1/2} \sum_{\mathbf{n}} \exp(i\mathbf{k}.\mathbf{n})\, \chi_\rho^{\mathbf{n}}(\mathbf{x}) \tag{2}$$

$$\chi_\rho^{\mathbf{n}}(\mathbf{x}) = \chi_\rho(\mathbf{x} - \mathbf{n} - \mathbf{r}) \tag{3}$$

where $\mathbf{k}$ is the wave vector, j the band index, $N^{-1/2}$ the normalizing coefficient. The sum $\sum_\rho$ extends to all the AO's centred in the R atom, whose coordinates are defined by the translation vector $\mathbf{n}$ (which gives the cell to which it belongs) and by the fractionary vector $\mathbf{r}$ (which gives the position it occupies in the reference cell). The sum $\sum_R$ extends to all the atoms in the unit cell.

Using a tight-binding set gives the Hamiltonian a block-diagonal structure with a $d \times d$ block for each $\mathbf{k}$ value $\left(d = \sum_R \sum_\rho 1\right)$. The $A^{\mathbf{k}}$ matrix of the $a_{\rho j}^{\mathbf{k}}$ coefficients is given by the Roothaan-like matrix equation $F^{\mathbf{k}} A^{\mathbf{k}} = S^{\mathbf{k}} A^{\mathbf{k}} E^{\mathbf{k}}$, to be solved by the SCF method.

The general elements of the overlap matrix and of the Hartree-Fock Hamiltonian matrix have the form :

$$S_{\rho\sigma}^{\mathbf{k}} = \sum_{\mathbf{n}} \exp(i\mathbf{k}.\mathbf{n}) \langle \chi_\rho^0 | \chi_\sigma^{\mathbf{n}} \rangle \tag{4}$$

$$F_{\rho\sigma}^{\mathbf{k}} = \sum_{\mathbf{n}} \exp(i\mathbf{k}.\mathbf{n}) \langle \chi_\rho^0 | \mathcal{H} | \chi_\sigma^{\mathbf{n}} \rangle + \sum_{\mathbf{n},\mathbf{n}',\mathbf{n}''} \sum_{\tau,\upsilon} \frac{1}{B} \int_B \mathrm{d}\mathbf{k}'\, P_{\tau\upsilon}(\mathbf{k}') \exp[i\mathbf{k}.\mathbf{n} + i\mathbf{k}'.(\mathbf{n}' - \mathbf{n}'')] \times$$

$$\times \left[\langle \chi_\rho^0 \chi_\tau^{\mathbf{n}'} | \mathcal{G} | \chi_\sigma^{\mathbf{n}} \chi_\upsilon^{\mathbf{n}''} \rangle - \frac{1}{2} \langle \chi_\rho^0 \chi_\tau^{\mathbf{n}'} | \mathcal{G} | \chi_\upsilon^{\mathbf{n}''} \chi_\sigma^{\mathbf{n}} \rangle \right] \tag{5}$$

where B refers to the first Brillouin zone.

The bond order matrix element is defined for each $\mathbf{k}$ by :

$$P_{\tau\upsilon}(\mathbf{k}) = 2 \sum_j a_{\tau j}^{\mathbf{k}}\, a_{\upsilon j}^{\mathbf{k}}\, \theta(\varepsilon_{\mathrm{F}} - \varepsilon_j^{\mathbf{k}}) \tag{6}$$

where ε_j^k is the jth diagonal element of the E^k matrix, ε_F the Fermi energy and θ the Heaviside step function.

The CNDO/2 approximation, as applied to the integrals in equations (4) and (5), gives :

$$\langle \chi_\rho^0 | \chi_\sigma^n \rangle = \delta_{\rho\sigma}\,\delta_{0n} \tag{7}$$

$$\langle \chi_\rho^0 | \mathcal{H} | \chi_\rho^0 \rangle = \frac{1}{2}(I_\rho + A_\rho) + \frac{1}{2}\gamma_R^\circ - \sum_T Z_T \sum_n \gamma_{RT}^{0n} \tag{8}$$

$$\langle \chi_\rho^0 | \mathcal{H} | \chi_\sigma^n \rangle = \frac{1}{2}(\beta_R^\circ + \beta_S^\circ)\langle \chi_\rho^0 | \chi_\sigma^n \rangle \qquad (\sigma \neq \rho \quad \text{and/or} \quad \mathbf{n} \neq \mathbf{0}) \tag{9}$$

$$\langle \chi_\rho^0 \chi_\tau^n | \mathcal{G} | \chi_\sigma^{n'} \chi_\upsilon^{n''} \rangle = \delta_{\rho\sigma}\,\delta_{\tau\upsilon}\,\delta_{0n'}\,\delta_{nn''}\,\gamma_{RT}^{0n} \tag{10}$$

where δ is the Kronecker symbol, I_ρ, A_ρ, γ_R°, β_R° are parameters entering the approximate expressions for one-electron integrals, Z_T is the core charge of the T atom, and γ_{RT}^{0n} is the Coulomb integral over the ρ° and τ° AO's of s type belonging to the valence shell of atoms R and T, respectively :

$$\gamma_{RT}^{0n} = \int \mathrm{d}\mathbf{x}_1\,\mathrm{d}\mathbf{x}_2 \frac{|\chi_{\rho^\circ}(\mathbf{x}_1 - \mathbf{r})|^2 \cdot |\chi_{\tau^\circ}(\mathbf{x}_2 - \mathbf{n} - \mathbf{t})|^2}{|\mathbf{x}_1 - \mathbf{x}_2|} \tag{11}$$

By applying the CNDO/2 approximation [4], the matrix equation changes to $F^k A^k = A^k E^k$ and the $F_{\rho\sigma}^k$ element becomes [3, 5] :

$$F_{\rho\sigma}^k = \delta_{\rho\sigma}\left\{ -\frac{1}{2}(I_\rho + A_\rho) + \frac{1}{2}\gamma_R^\circ - \beta_R^\circ + \sum_T J_{RT}\left[\sum_\tau \frac{1}{B}\int_B \mathrm{d}\mathbf{k}'\, P_{\tau\tau}(\mathbf{k}') - Z_T\right]\right\} +$$

$$+ \frac{1}{2}(\beta_R^\circ + \beta_S^\circ)\sum_n \exp(i\mathbf{k}\cdot\mathbf{n})\langle \chi_\rho^0 | \chi_\sigma^n \rangle\rangle \; - \frac{1}{2B}\int_B \mathrm{d}\mathbf{k}'\, P_{\rho\sigma}(\mathbf{k}')\, K_{RS}(\mathbf{k} + \mathbf{k}') \tag{12}$$

where :

$$J_{RT} = \sum_n \gamma_{RT}^{0n} \tag{13}$$

$$K_{RS}(\mathbf{k} + \mathbf{k}') = \sum_n \exp[i(\mathbf{k} + \mathbf{k}')\cdot\mathbf{n}]\gamma_{RS}^{0n} \tag{14}$$

The difference $\left[\sum_\tau \frac{1}{B}\int_B \mathrm{d}\mathbf{k}'\, P_{\tau\tau}(\mathbf{k}') - Z_T\right]$ in equation (12) gives the net electron charge q_T on the T atom in the NDO approximation, and the exchange term in the same equation can be expanded in a Fourier series :

$$\frac{1}{2B}\int_B \mathrm{d}\mathbf{k}'\, P_{\rho\sigma}(\mathbf{k}')\, K_{RS}(\mathbf{k} + \mathbf{k}') = \frac{1}{2}\sum_n \gamma_{RS}^{0n}\, p_{\rho\sigma}^n \exp(i\mathbf{k}\cdot\mathbf{n}) \tag{15}$$

$$p_{\rho\sigma}^n = \frac{1}{B}\int_B \mathrm{d}\mathbf{k}'\, P_{\rho\sigma}(\mathbf{k}') \exp(i\,\mathbf{k}'\cdot\mathbf{n}) \tag{16}$$

so that $F_{\rho\sigma}^k$ can be rewritten in the form :

$$F_{\rho\sigma}^k = \delta_{\rho\sigma}\left\{ -\frac{1}{2}(I_\rho + A_\rho) + \frac{1}{2}\gamma_R^\circ - \beta_R^\circ + \sum_T q_T J_{RT}\right\} + \sum_n \left[\frac{1}{2}\left(\beta_R^0 + \beta_S^0\right)\langle \chi_\rho^0 | \chi_\sigma^n \rangle - \frac{1}{2}\, p_{\rho\sigma}^n\, \gamma_{RS}^{0n}\right] \exp(i\mathbf{k}\cdot\mathbf{n}) \tag{17}$$

Contributions from the last sum decrease rapidly with $|\mathbf{n}|$, becoming negligible beyond a few atomic units, so that there is no problem in truncation. More attention must be paid to the Coulomb term entering the diagonal $F_{\rho\rho}^k$ element.

Since the difference $[\gamma_{RT}^{0n} - v_{rtn}^{-1}]$, where

$$v_{rtn} = |\mathbf{n} + \mathbf{t} - \mathbf{r}| \tag{18}$$

rapidly vanishes with increasing $|\mathbf{n}|$, we may subdivide the sum over $\mathbf{n}$ into two parts, according to the applicability or non-applicability of the approximation $\gamma_{RT}^{0\mathbf{n}} \cong v_{rtn}^{-1}$:

$$J_R = \sum_T q_T J_{RT} = \sum_{\substack{\mathbf{n} \\ (|\mathbf{n}| \leq n_0)}} \sum_T q_T \gamma_{RT}^{0\mathbf{n}} + \sum_{\substack{\mathbf{n} \\ (|\mathbf{n}| > n_0)}} \sum_T \frac{q_T}{v_{rtn}} = J_1(\mathbf{r}) + J_2(\mathbf{r}) \tag{19}$$

It is easily seen that $\sum_T \frac{q_T}{v_{rtn}}$ is the potential generated at $\mathbf{r}$ by the distribution of point charges q_T corresponding to the position of the various atoms in the $\mathbf{n}$ th cell. But this is also the potential $V(\mathbf{r}-\mathbf{n})$ generated at $(\mathbf{r}-\mathbf{n})$ by the same distribution of charges in the reference cell at the origin, so that we have :

$$J_2(\mathbf{r}) = \sum_{\mathbf{n}}'' V(\mathbf{r}-\mathbf{n}) \tag{20}$$

where $\sum_{\mathbf{n}}''$ extends to all the cells with $|\mathbf{n}| > n_0$ (while $\sum_{\mathbf{n}}'$ will indicate the sum extending to all the cells with $|\mathbf{n}| \leq n_0$). Then $J_2(\mathbf{r})$ can be written using a multipole expansion of that charge distribution [6] :

$$J_2(\mathbf{r}) = \sum_{l,m}' \rho_l^m G_l^m(\mathbf{r}) \tag{21}$$

$$G_l^m(\mathbf{r}) = \left(\frac{4\pi}{2l+1}\right)^{1/2} \sum_{\mathbf{n}}'' Y_l^m(\theta_{\mathbf{n}}', \varphi_{\mathbf{n}}') \cdot |\mathbf{r}-\mathbf{n}|^{-(l+1)} \tag{22}$$

$$\rho_l^m = \left(\frac{4\pi}{2l+1}\right)^{1/2} \sum_T q_T Y_l^m(\theta_t, \varphi_t) \cdot |\mathbf{t}|^l . \tag{23}$$

The sum $\sum_{l,m}'$ is for $\sum_{l=1}^{\infty} \sum_{m=-l}^{l}$, the term $l = 0$ being excluded in equation (21) because of the neutrality condition $\rho_0^0 = \sum_T q_T = 0$. In equation (22), $\theta_{\mathbf{n}}'$ and $\varphi_{\mathbf{n}}'$ refer to the vector $(\mathbf{r}-\mathbf{n})$.

Furthermore, $G_l^m(\mathbf{r})$ can be expressed as a power series of the auxiliary variable $(|\mathbf{r}|/|\mathbf{n}|)$:

$$G_l^m(\mathbf{r}) = \sum_{\mathbf{n}}'' |\mathbf{n}|^{-(l+1)} \sum_{j=0}^{\infty} g_{l,j}^m(\theta_{\mathbf{n}}, \varphi_{\mathbf{n}}\,;\, \theta_{\mathbf{r}}, \varphi_{\mathbf{r}}) (|\mathbf{r}|/|\mathbf{n}|)^j \tag{24}$$

where the $g_{l,j}^m$ coefficients can be obtained by identifying polynomials between equations (22) and (24), so that, by considering $J_R' = J_R - J_2(\mathbf{0})$, one obtains :

$$J_R' = J_1(\mathbf{r}) + \sum_{l,m}' [G_l^m(\mathbf{r}) - G_l^m(\mathbf{0})] \rho_l^m = J_1(\mathbf{r}) + \sum_{l,m}' \rho_l^m \sum_{\mathbf{n}}'' \sum_j' g_{l,j}^m |\mathbf{r}|^j |\mathbf{n}|^{-(l+j+1)} \tag{25}$$

where $\sum_j' = \sum_{j=1}^{\infty}$.

It is seen from this expression that the terms in the second part of J_R' are proportional to $|\mathbf{n}|^{-(l+j+1)}$, the lowest order term ($l = j = 1$) vanishing with $|\mathbf{n}|^{-3}$. If N_0 is chosen large enough for $\sum_{\substack{\mathbf{n} \\ (|\mathbf{n}| > N_0)}}$ to be substituted by an integral, the overall contribution from outer cells is easily calculated. In conclusion the differences $[G_l^m(\mathbf{r}) - G_l^m(\mathbf{0})]$ behave like structure factors which may be evaluated once and for all, while the spherical multipole moments ρ_l^m are easily calculated at each stage in the SCF procedure. The choice of the cluster of cells with $|\mathbf{n}| \leq n_0$, for which the correct expression of $\gamma_{RT}^{0\mathbf{n}}$ must be taken into account, and that of the shell of cells with $n_0 < |\mathbf{n}| \leq N_0$ for which contributions to the structure factors must be directly summed up, is a matter of convenience.

Using J_R' instead of J_R obviously gives a new F' matrix, which requires a new expression for the total energy [7] :

$$E = E' - \frac{1}{2} \sum_R \sum_{l,m}' [G_l^m(\mathbf{r}) - G_l^m(\mathbf{0})] \rho_l^m \tag{26}$$

Eigenvectors are not affected, however, since $J_2(\mathbf{0})$ is subtracted from all the diagonal elements in the Hartree-Fock matrix ($F' = F - J_2(\mathbf{0}) \cdot I$), so that the A matrix is unchanged.

By interpreting the NDO approximation as a Löwdin orthogonalization, the A' matrix corresponding to the non-orthogonal basis set can be obtained simply by putting $A' = S^{-1/2} A$. This treatment, which applies to crystals as well as to molecules [8], enables us to define new coefficients :

$$a'^{\mathbf{k}}_{\rho j} = (A')^{\mathbf{k}}_{\rho j} = \sum_{T,Y} \sum_{\tau,\upsilon} (U^{\mathbf{k}})_{\rho\tau} [(\Lambda^{\mathbf{k}})_{\tau\tau}]^{-1/2} (U^{\mathbf{k}})^*_{\upsilon\tau} (A^{\mathbf{k}})_{\upsilon j} \tag{27}$$

where $U^{\mathbf{k}}$ is the unitary matrix which diagonalizes $S^{\mathbf{k}}$, and $\Lambda^{\mathbf{k}}$ is the corresponding diagonal matrix.

Using the Dirac δ-function the total number of electrons may now be written :

$$n = 2 \int \mathrm{d}\varepsilon \int \mathrm{d}\mathbf{k} \int \mathrm{d}\mathbf{x} \theta(\varepsilon_F - \varepsilon) \sum_{R,S} \sum_{\rho,\sigma} \sum_{\mathbf{n},\mathbf{n}'} \sum_{j} \delta(\varepsilon - \varepsilon^{\mathbf{k}}_j)\, a'^{\mathbf{k}*}_{\rho j}\, a'^{\mathbf{k}}_{\sigma j} \exp[i\mathbf{k} \cdot (\mathbf{n} - \mathbf{n}')]\, \chi^{\mathbf{n}'}_{\rho}(\mathbf{x})\, \chi^{\mathbf{n}}_{\sigma}(\mathbf{x}) \tag{28}$$

The electron charge distribution in real space is obtained by integration over the reciprocal space and over the energy in each band, and by summation over those j values which correspond to energies below the Fermi level :

$$\rho(\mathbf{x}) = \sum_{R,S} \sum_{\rho,\sigma} \sum_{\mathbf{n},\mathbf{n}'} P^{\mathbf{n}-\mathbf{n}'}_{\rho\sigma}\, \chi^{\mathbf{n}'}_{\rho}(\mathbf{x})\, \chi^{\mathbf{n}}_{\sigma}(\mathbf{x}) \tag{29}$$

$$P^{\mathbf{n}-\mathbf{n}'}_{\rho\sigma} = 2 \int \mathrm{d}\mathbf{k} \sum_{\substack{j \\ (\varepsilon^{\mathbf{k}}_j \leqslant \varepsilon_F)}} a'^{\mathbf{k}*}_{\rho j}\, a'^{\mathbf{k}}_{\sigma j} \exp[i\mathbf{k} \cdot (\mathbf{n} - \mathbf{n}')] \tag{30}$$

Integration in real space can be carried out by separately considering contributions from different pairs of AO's :

$$n^{\mathbf{n}\mathbf{n}'}_{\rho\sigma} = \int \mathrm{d}\mathbf{x} P^{\mathbf{n}-\mathbf{n}'}_{\rho\sigma}\, \chi^{\mathbf{n}'}_{\rho}(\mathbf{x})\, \chi^{\mathbf{n}}_{\sigma}(\mathbf{x}) = P^{\mathbf{n}-\mathbf{n}'}_{\rho\sigma}\, S^{\mathbf{n}-\mathbf{n}'}_{\rho\sigma} \tag{31}$$

where, for a given couple of AO's, both P and S only depend on the relative position of the corresponding cells. These single pair contributions then may be grouped according to the Mulliken scheme for population analysis, giving bond populations and atomic charges :

$$q^{\mathbf{n}\mathbf{n}'}_{RS} = 2 \sum_{\rho,\sigma} n^{\mathbf{n}\mathbf{n}'}_{\rho\sigma} \tag{32}$$

$$q_R = \sum_{\rho} n^{\mathbf{0}\mathbf{0}}_{\rho\rho} \tag{33}$$

$$Q_R = q_R + \frac{1}{2} \sum_{\mathbf{n}} \sum_{S}{}' q^{\mathbf{0}\mathbf{n}}_{RS} \tag{34}$$

where the R atom in the 0th cell is excluded in $\sum_S{}'$.

The density of states $\rho(\varepsilon)$, which obviously obeys the condition :

$$\int \mathrm{d}\varepsilon \theta(\varepsilon_F - \varepsilon)\, \rho(\varepsilon) = n \tag{35}$$

is obtained by integration over both the reciprocal and real space, and by summation over all the bands (the restriction $\varepsilon \leqslant \varepsilon_F$ being removed) :

$$\rho(\varepsilon) = \sum_{R,S} \sum_{\rho,\sigma} \sum_{\mathbf{n},\mathbf{n}'} P'^{\mathbf{n}-\mathbf{n}'}_{\rho\sigma}\, S^{\mathbf{n}-\mathbf{n}'}_{\rho\sigma} \tag{36}$$

$$P'^{\mathbf{n}-\mathbf{n}'}_{\rho\sigma}(\varepsilon) = 2 \int \mathrm{d}\mathbf{k} \sum_{j} \delta(\varepsilon - \varepsilon^{\mathbf{k}}_j)\, a'^{\mathbf{k}*}_{\rho j}\, a'^{\mathbf{k}}_{\sigma j} \exp[i\mathbf{k} \cdot (\mathbf{n} - \mathbf{n}')] \,. \tag{37}$$

Partial contributions $P'^{\mathbf{n}-\mathbf{n}'}_{\rho\sigma} \cdot S^{\mathbf{n}-\mathbf{n}'}_{\rho\sigma}$ again may be grouped according to a Mulliken-like scheme, giving the corresponding *projected* densities of states.

3. **Atomic hydrogen chemisorbed on graphite.** — The regular phases here considered are schematically shown in figure 1, together with the corresponding Brillouin zones and their irreducible parts. Surface compositions of the various phases are indicated in brackets and point groups of the surface lattices are also given.

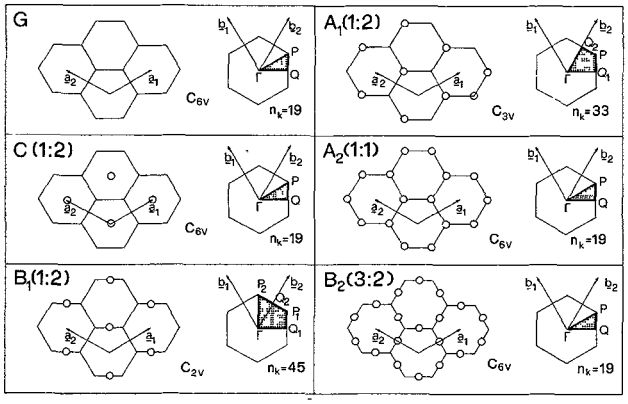

FIG. 1. — Surface configurations of different chemisorbed phases and related Brillouin zones. Letters characterize the adsorption site : C = centre of the ring ; A = carbon atom ; B = C-C bond. G is for the reference graphite monolayer. Hydrogen/carbon atomic ratios are given in brackets. Grey areas show the irreducible part of the Brillouin zones for the various point groups of the crystal, and n_k gives the number of sampling points considered in each case.

Calculations have been performed using $n_0 \cong 15$ a.u. (central cluster of 25 cells) and $N_0 \cong 30$ a.u.

Integrations in the reciprocal space, which are needed for evaluating Fermi energy and the elements in the H-F Hamiltonian at each stage in the SCF procedure are carried out by taking full advantage of the symmetry properties of the system and by using suitable interpolating functions to fit the values calculated for a set of sampling points. Sampling has been effected using in all cases a commensurate net of triangular meshes, with side length $b/12$, b being the modulus of the reciprocal lattice translation. The different shapes of the irreducible part of the Brillouin zone, involved by the different symmetry properties of the various phases, require a different number n_k of sampling points to be considered, which is also given in figure 1. Local triangular domains have been considered for interpolation, with sides twice as large as the meshes of the commensurate net ; for each of such domains the integrand function has been approximated by a full quadratic function.

The two-dimensional character of chemisorbed phases, and the quadratic form of the locally interpolating functions allow the evaluation of the number of states with energy below the Fermi level to be carried out analytically even in cases where the bands are cut by the Fermi surface (conducting systems). As far as integrals of the form $\int_B \mathrm{d}\mathbf{k} P_{\rho\sigma}(\mathbf{k}) \cdot \mathbf{F}(\mathbf{k})$ are concerned, where discontinuities in the elements of the bond order matrix at the Fermi surface must be taken into account for conducting systems, the discontinuous function $P_{\rho\sigma}(\mathbf{k})$ has been approximated in each interpolation domain by the continuous function :

$$P'_{i,\rho\sigma}(\mathbf{k}) = 2 \sum_j a^{\mathbf{k}*}_{\rho j} a^{\mathbf{k}}_{\sigma j} s_{ij} \qquad (38)$$

where the sum extends over the different bands and s_{ij} is the previously calculated surface fraction of the ith domain with $\varepsilon_j < \varepsilon_F$ [9].

Using the above approximations, the total energy proved to converge within 10^{-2} hartrees, which is usually enough for conformational studies. Equilibrium conditions have been determined by minimizing the energy with respect to all the geometrical parameters which are needed for defining the structure of the phase formed on chemisorption, so involving substrate relaxation [7, 8, 10].

The results obtained in this way are shown by the data in table I and by the band structures and density of states spectra in figures 4 to 13. The band structure of the graphite monolayer, as obtained in

TABLE I.

Chemisorption data for atomic hydrogen on graphite. (Symbols for different phases as in Fig. 1).

C	$E =$ + 0.92 eV	$Q_C =$ 3.99
	$\Delta E =$ 0.06 eV	$Q_H =$ 1.02
	C-H = 0.90 Å	$q_{C\text{-}H} =$ − 0.04
	C-C = 1.43 Å	$q_{C\text{-}C} =$ 0.98
A_1	$E =$ − 1.35 eV	$Q_{C_1} =$ 4.10
	$\Delta E =$ 0.46 eV	$Q_{C_2} =$ 3.95
		$Q_H =$ 0.95
	C-H = 1.15 Å	$q_{C\text{-}H} =$ 0.40
	C-C = 1.43 Å	$q_{C\text{-}C} =$ 0.90
	$\theta =$ 93.6°	
A_2	$E =$ − 3.30 eV	$Q_C =$ 3.97
	$\Delta E =$ 0.68 eV	$Q_H =$ 1.03
	C-H = 1.14 Å	$q_{C\text{-}H} =$ 0.66
	C-C = 1.51 Å	$q_{C\text{-}C} =$ 0.86
B_1	$E =$ − 1.79 eV	$Q_C =$ 4.02
	$\Delta E =$ 0.47 eV	$Q_H =$ 0.96
	C-H = 1.07 Å	$q_{C\text{-}H} =$ 0.18
	C-C = 1.51 Å	$q_{C\text{-}C} =$ 0.68
	(C-C) = 1.44 Å	$q_{C\text{-}C'} =$ 1.00
	$\varphi =$ 117.6°	
B_2	$E =$ − 0.51 eV	$Q_C =$ 3.97
	$\Delta E =$ 0.88 eV	$Q_H =$ 1.02
	C-H = 1.10 Å	$q_{C\text{-}H} =$ 0.12
	C-C = 1.53 Å	$q_{C\text{-}C} =$ 0.76

E = adsorption energy per adsorbed atom ; ΔE = relaxation energy per adsorbed atom ; Q_X = gross atomic charge of X atom ; $q_{X\text{-}Y}$ = overlap population in the X-Y bond ; θ = HĈC in A_1 phase ; φ = C(ĈH)C in B_1 phase. C_2 refers to the carbon bound to hydrogen in A_1 ; C-C and (C-C) refer to bonds with and without adsorbed hydrogen atom in B_1. E is obtained from the difference between the total energy of the relaxed system in its equilibrium configuration and that of the graphite monolayer plus the isolated hydrogen atoms. ΔE is obtained by difference from phases having the same composition and surface configuration, with relaxed or unrelaxed substrate.

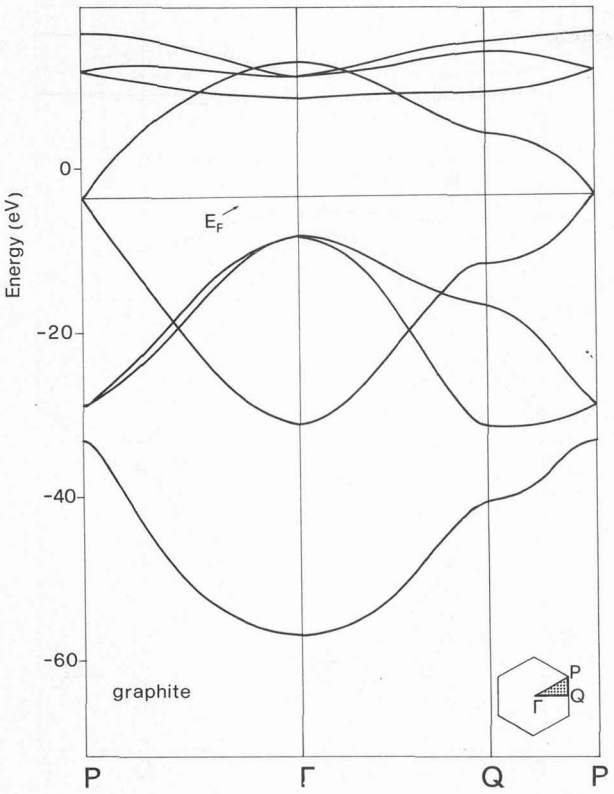

FIG. 2. — Band structure for the graphite monolayer. In this and in the following figures, the contour is shown by the scheme bottom right.

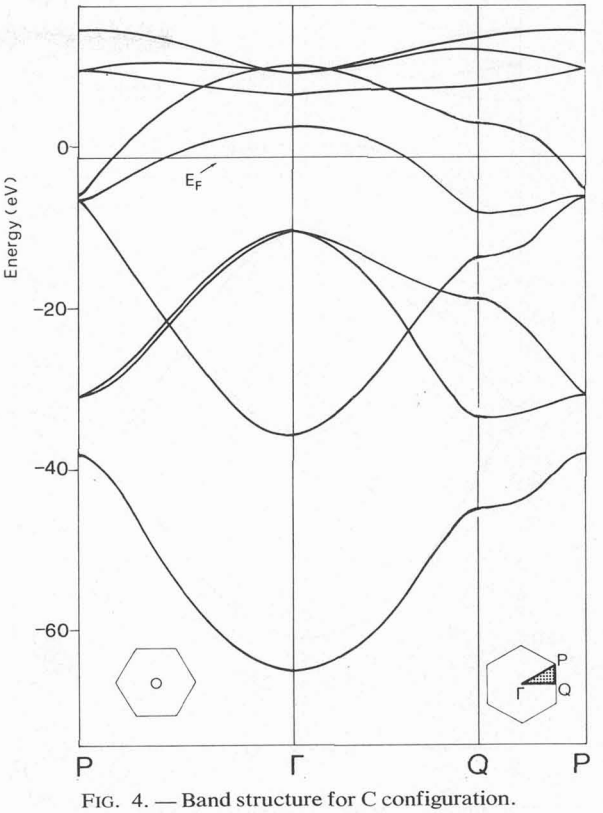

FIG. 4. — Band structure for C configuration.

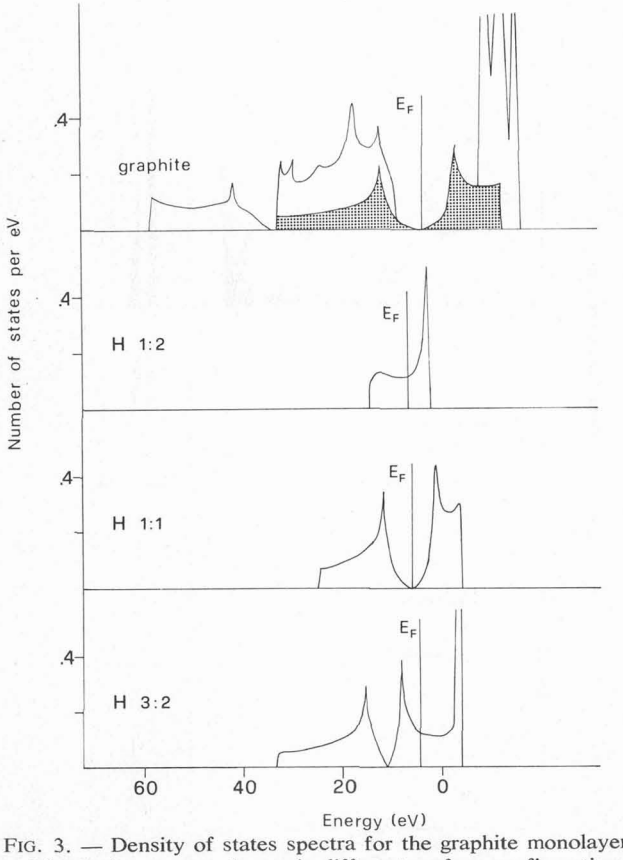

FIG. 3. — Density of states spectra for the graphite monolayer and for hydrogen monolayers in different surface configurations (relaxation not taken into account). The grey area in the graphite spectrum refers to 2 p_z AO's contribution. The H(1:2) spectrum is common to the hydrogen monolayer in cases C, A_1, B_1.

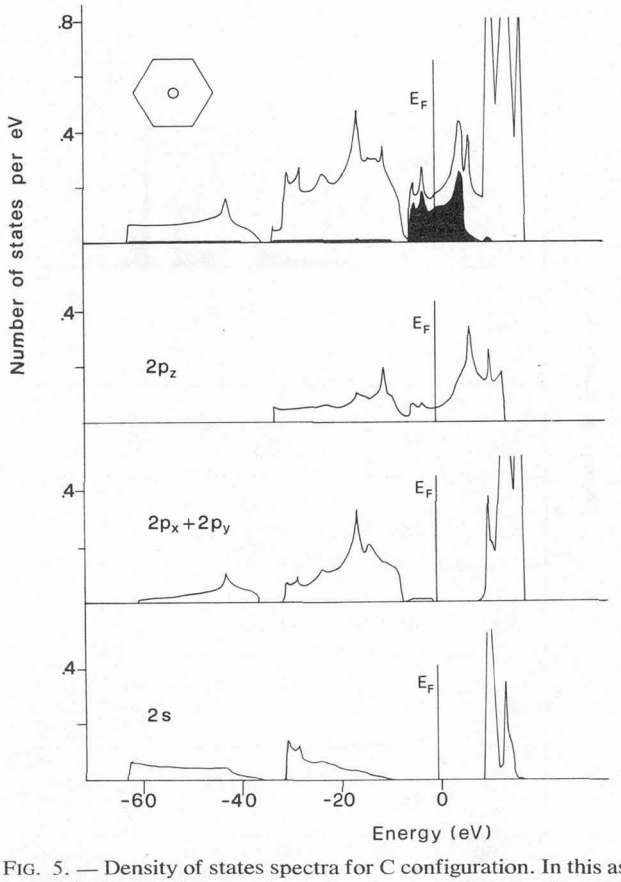

FIG. 5. — Density of states spectra for C configuration. In this as in the following figures, the top spectrum refers to the total density of states, with the 1s hydrogen contribution in black. Partial contributions from different carbon AO's are given in the other spectra.

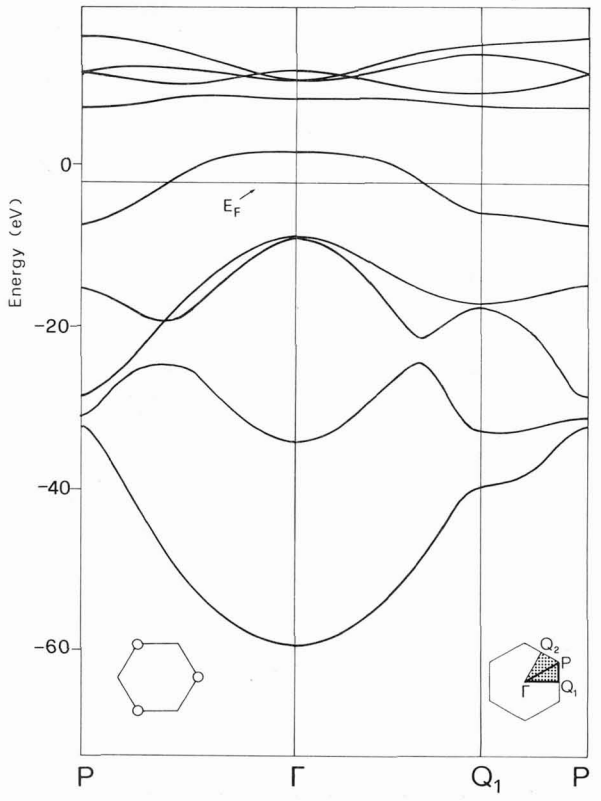

FIG. 6. — Band structure for A_1 phase.

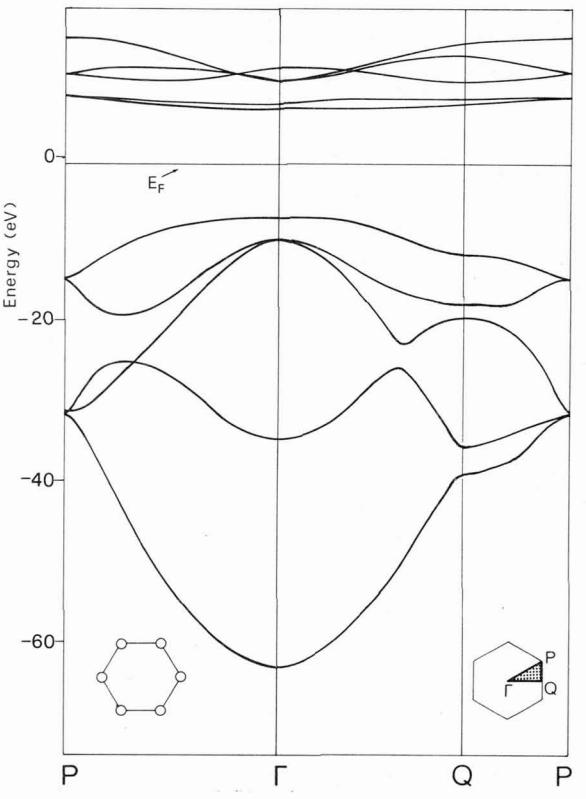

FIG. 8. — Band structure for A_2 phase.

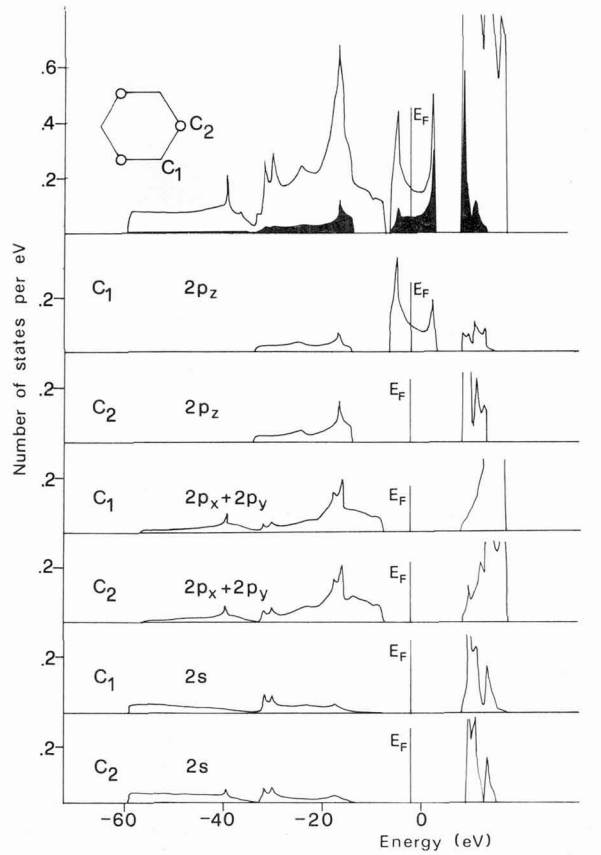

FIG. 7. — Density of states spectra for A_1 phase. Contributions from AO's belonging to the two non-equivalent carbon atoms are reported separately.

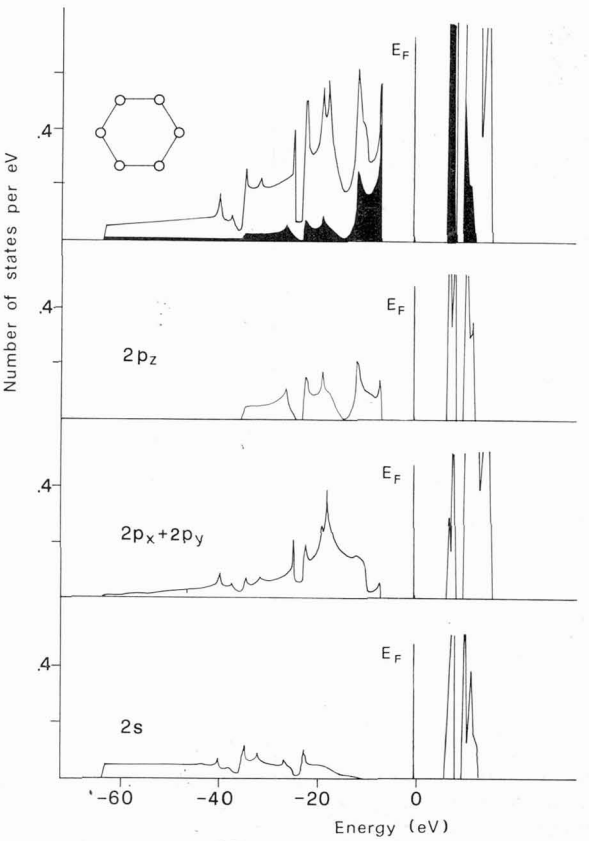

FIG. 9. — Density of states spectra for A_2 phase.

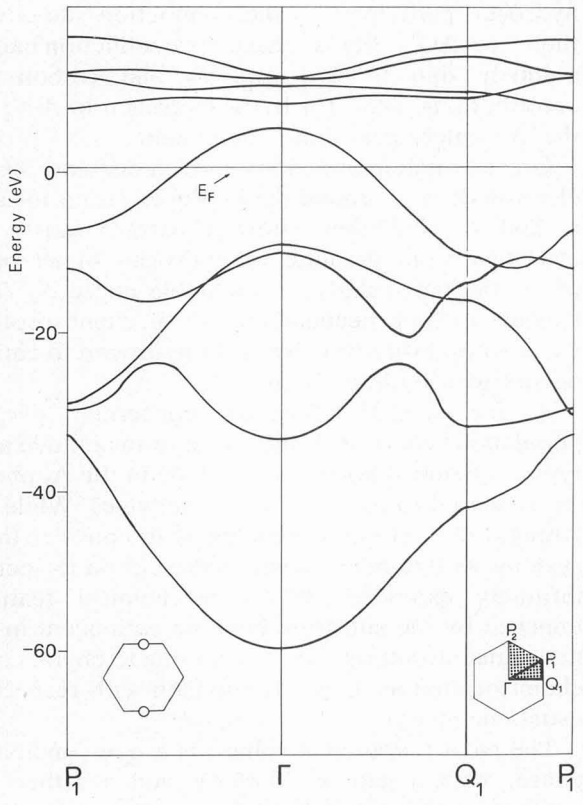

FIG. 10. — Band structure for B_1 phase.

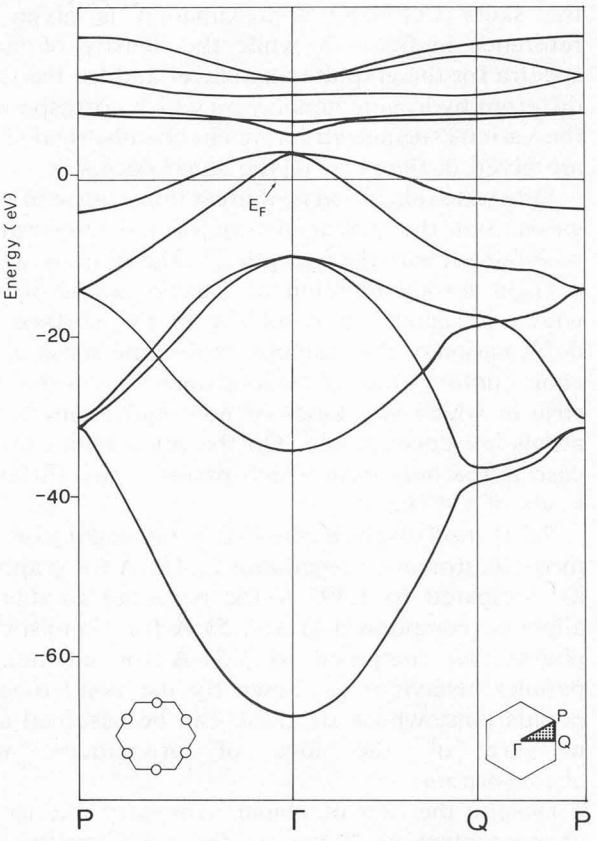

FIG. 12. — Band structure for B_2 phase.

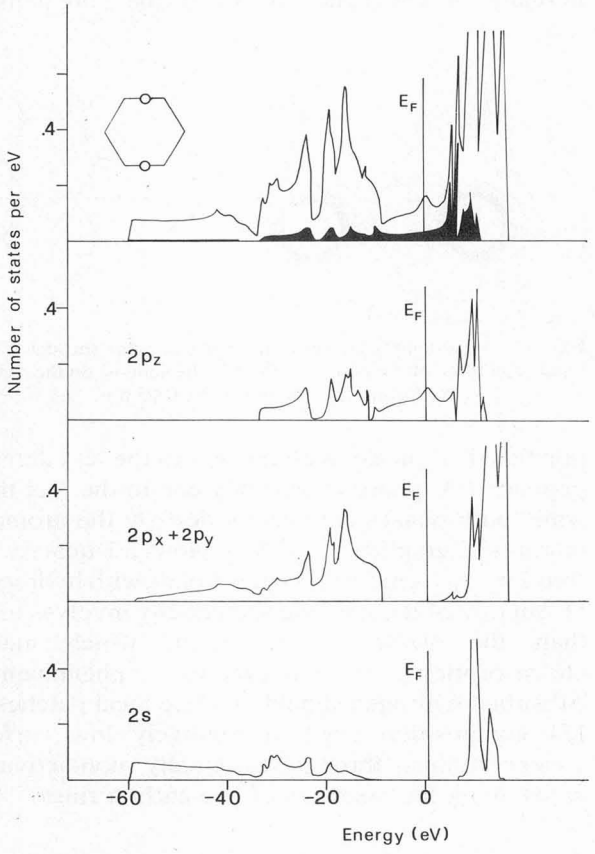

FIG. 11. — Density of states spectra for B_1 phase.

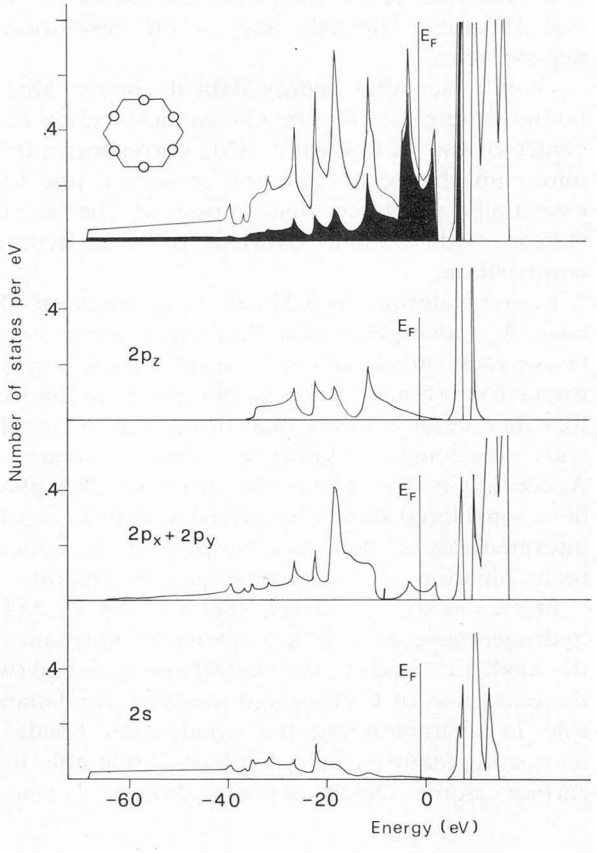

FIG. 13. — Density of states spectra for B_2 phase.

the same CO-NDO approximation is given for reference in figure 2, while the density of states spectra for the graphite monolayer and for the three different hydrogen monolayers which correspond to the various surface structures in chemisorbed states are given in figure 3 for the same purposes.

Substrate relaxation is of great importance in most cases, but the planar nature of the substrate is maintained, with the exception of the A_1 case, where a slight tetrahedrization of carbon atoms occurs, which introduces a wrinkling in the surface, by deformation of the graphite rings in the sense of the chair conformation of cyclohexane. This is the only case in which two kinds of non equivalent carbon atoms are encountered. On the other hand, the B_2 case is the only case which presents two different kinds of C-C bonds.

Relaxation displaces the C-C bond length from the range of aromatic compounds (1.415 Å for graphite, as compared to 1.395 Å for benzene) to that of aliphatic compounds (1.51-1.53 Å for chemisorbed phases, as compared to 1.54 Å for ethane). A parallel behaviour is shown by the bond overlap populations, whose decrease can be assumed as a measure of the loss of aromaticity with chemisorption.

Despite the loss of planar symmetry due to the chemisorption of hydrogen, the band structure of the various phases still reminds us of the graphite band structure, with obvious changes in the shape and extension of the bands due to the mixing of C and H atomic orbitals and to the resolution of degeneracies.

From adsorption energy data it appears that no bound state exists for the C case (adsorption at the centre of the carbon ring). This corresponds to the minimum change in the band structure, and to an essentially unaltered distribution of the electron states, with simple overlap of the hydrogen contribution.

Bound states are found in all the other cases. Only case A_2 (adsorption of a hydrogen atom directly above each carbon atom of the substrate), however, seems to correspond to a stable phase, in the sense that its energy is lower than the energy of graphite and molecular hydrogen taken separately. According to this result the other surface phases here considered should be looked at only as possible intermediates in chemical adsorption or in molecular recombination of atomic hydrogen on graphite.

From density of states spectra, the 1s AO of hydrogen appears to give a relevant contribution to the modified bands in the central energy range (with the exception of C case) and to play a fundamental role in characterizing the conduction band. An interesting feature of the A_1 phase is that only those carbon atoms which are not directly bound to hydrogen participate in the conduction states with their $2p_z$ AO's. For B_1 phase the conduction band is uniquely due to hydrogen 1s and carbon $2p_z$ contributions, while for B_2 the hydrogen 1s AO's are the absolutely prevailing component.

Gross atomic populations show a decrease of the electron density around the hydrogen atoms in cases C and A_1, but they show a partial transfer of electrons from graphite to hydrogen in all other cases and particularly in the stable phase A_2. This appears to be a peculiar feature of chemisorption, since an opposite transfer from hydrogen to carbon occurs with hydrocarbons.

As far as C-H bonds are concerned, overlap populations are of the same order of magnitude as in typical chemical bonds ($q_{C\text{-}H} = 0.66$ in the A_2 phase, as compared to $q_{C\text{-}H} = 0.78$ for methane). While the strength of C-H bonds enables us to consider these systems as two-dimensional hydrocarbon molecules infinitely extended, the stereochemical features imposed by the substrate have no equivalent in the molecular structures, so contributing to characterize chemisorption as a specific domain with respect to usual chemistry.

The most favoured A_2 phase is a non-conducting phase, with a gap of 10.36 eV and a rather flat valence band, which reflects the essentially localized nature of corresponding electrons. In fact localization occurs in the sharply defined C-H bonds which are well described by the electron density map in figure 14. The higher stability of the more densely

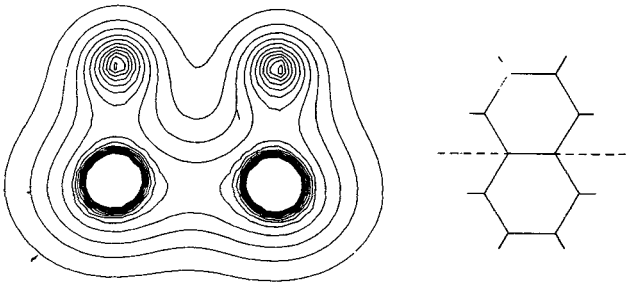

FIG. 14. — Isodensity curves in the vertical plane through a C-C bond. The trace of the plane is shown in the scheme on the right in the figure. Increments are by 0.05 a.u.

populated A_2 phase, with respect to the less densely populated A_1 phase is probably due to the fact that, while both phases completely destroy the aromatic features of graphite, only A_2 exploits adequately the free $2p_z$ AO's in forming new bonds with hydrogen. Disrupture of the graphite aromaticity involves more than the single carbon atom, which makes chemisorption a cooperative phenomenon. Adsorbed hydrogen should produce local patches of 1/1 composition even at relatively low surface concentrations, through essentially non-activated paths along the contours of the carbon rings.

References

[1] PEACOCK, T. E. and MCWEENY, R., *Proc. Phys. Soc. London* **74** (1959) 385.
[2] ANDRÉ, J. M., GOUVERNEUR, L. and LEROY, G., *Int. J. Quantum Chem.* **1** (1967) 427, 451.
[3] DOVESI, R., PISANI, C., RICCA, F. and ROETTI, C., *Chem. Phys. Lett.* **39** (1976) 103.
[4] POPLE, J. A. and BEVERIDGE, D. L., *Approximate Molecular Orbital Theory* (McGraw-Hill, New York) 1970.
[5] DOVESI, R., PISANI, C., RICCA, F. and ROETTI, C., *J. Chem. Phys.* **65** (1976) 3075.
[6] BUCKINGHAM, A. D., *Q. rev.* **13** (1959) 183.
[7] DOVESI, R., PISANI, C., RICCA, F. and ROETTI, C., accepted for publication in *Surf. Sci.*
[8] DOVESI, R., PISANI, C., RICCA, F. and ROETTI, C., *J. Chem. Phys.* **65** (1976) 4116.
[9] CHIONO, M., PISANI, C., RANGHINO, G. and ROETTI, C., *Gazz. Chim. Ital.* **106** (1976) 921.
[10] DOVESI, R., PISANI, C., RICCA, F. and ROETTI, C., *Chem. Phys. Lett.* **44** (1976) 104.

DISCUSSION

J. G. DASH. — Could you comment on the fact that H_2 and O_2 apparently do not dissociate on the basal plane of graphite ?

F. RICCA. — Different explanations can be given for the lack of experimental evidence concerning dissociation of molecular hydrogen on graphite. The first and less optimistic one, is that the approximations introduced in the above treatment are too unrealistic, so that even the relative calculated energies are not correct. To be a bit more confident, however, other possible reasons could be discovered. The essential one is that chemisorption could require disrupting the *aromatic* character of graphite, which involves a very high activation energy. It is perfectly possible that the high temperatures required for such an activation correspond to an entropy term which is sufficient to practically annihilate the process. Furthermore, at such high temperatures, it looks quite probable that other processes, like for instance the graphite demolition which proceeds from edges and defects, are completely obscuring the one we are searching for. It is well known, in fact, that CH_4 can be obtained from high temperature interaction between graphite and atomic hydrogen.

J. VILLAIN. — 1) You have spoken about infinite adsorbed films. Are these results for one single adsorbed atom ? If yes, how do they compare ?

F. RICCA. — Very preliminary results have just been obtained by Dr. Pisani, for a single hydrogen atom chemisorbed over a carbon atom of an infinite graphite monolayer, in the embedded cluster approach. We may not be sure, for the moment, that the evaluated energies can be properly compared ; it appears, however, that the energy obtained for such a band is intermediate between those previously calculated for the 1/2 and 1/1 regular phases.

2) Can you give a simple explanation for the difference between adsorption of O and H ? Is it a size effect ?

F. RICCA. — Differences between hydrogen and oxygen adsorption are in no way reducible to simple size effects. To discuss those differences, an accurate analysis of changes occurring in the energy band structure of graphite and in the distribution of states density is required, which will be done in a future paper.